(26) Vonk, C. G. *J. Appl. Crystallogr.* **1973**, *6*, 148.
(27) Jellinek, H. H. G. *Degradation of Vinyl Polymers*; Academic Press: New York, 1955.
(28) Miller, N. D.; Williams, D. F. *Biomaterials* **1987**, *8*, 129.
(29) Holland, S. J.; Jolly, A. M.; Yasin, M.; Tighe, B. J. *Biomaterials* **1987**, *8*, 289.

Thermal Isomerization Behaviors of a Spiropyran in Bilayers Immobilized with a Linear Polymer and a Smectitic Clay

Takahiro Seki* and Kunihiro Ichimura

Research Institute for Polymers and Textiles, 1-1-4 Higashi, Tsukuba, Ibaraki 305, Japan.
Received January 20, 1989; Revised Manuscript Received May 11, 1989

ABSTRACT: Thermal isomerization kinetics of photoinduced merocyanine to spiropyran is investigated in solid films having multibilayer structures, which consists of ion complexes between an ammonium bilayer forming amphiphile and polyanions. The reaction rates in these films abruptly increase near the crystal to liquid-crystal phase-transition temperature of the immobilized bilayer due to increased matrix mobility. The bilayer film immobilized with a smectitic silicate instead of a linear polymer provides more homogeneous reaction environments for the isomerizing chromophore and gives rise to a larger rate change at the phase-transition temperature. These improved properties by use of the clay is correlated to the increased order of bilayer structures in the film.

Introduction

The photochromic reaction of spiropyrans provides useful information on the dynamics of matrices as widely investigated in amorphous polymer solid films.[1] The reaction rate, which is frequently evaluated for the thermal reaction kinetics (isomerization of UV-induced merocyanine (PMC) → spiropyran (SP), scheme shown below),

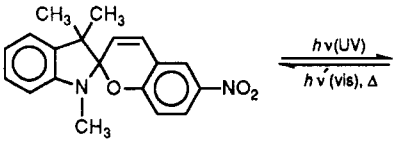

SP (1)

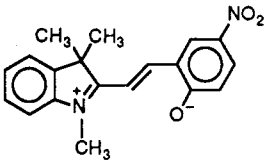

PMC

is dependent on the mobility of the surroundings and, in polymer matrices, is influenced by the glass transition. The sensitivity of the reaction to matrices can be ascribed to large changes of the molecular shape between the isomers. Studies on photochromic reaction behaviors and their controls in solid media have potential significances for practical applications such as optical recording.

More recently matrix effects for this reaction have been explored in media having ordered structures such as thermotropic[2] and lyotropic[3] liquid crystals, bilayer membranes,[4-7] and Langmuir-Blodgett (LB) multilayers.[8-12] Studies in such ordered matrices have advantages that reaction behaviors may be understood from physicochemical properties on the molecular level. We have reported the photochromic behaviors of spiropyrans incorporated into ammonium-type bilayer membranes dispersed in water,[5-7] particularly focusing on the effect of the fluidity change, i.e., the crystal to liquid-crystal phase transition (the temperature, T_c).

Kunitake and his co-workers have proposed simple casting methods for immobilization of bilayers to obtain transparent thin solid films.[13-16] The cast films have multibilayered structures similar to those of Y-type films prepared in the LB technique,[15,16] and the films maintain the phase-transition behaviors of aqueous bilayers.[13-15,17,18] Our present attention is focused on the photochromic behavior of spiropyrans embedded in such solid bilayer-immobilized films. This paper describes the thermal isomerization behavior of a spiropyran **1** (in the scheme) embedded in cast bilayer films composed of ion complexes between dioctadecyldimethylammonium and polyanions. Our preliminary report has shown abrupt rate changes in the thermal reaction brought about by the crystal to liquid-crystal phase transition of the immobilized bilayer complexed with poly(styrene sulfonate) (PSS).[19] In this work polyanions of two different types are employed as "bilayer binders", a linear polymer (PSS) and a two-dimensional smectitic clay (montmorillonite, Mont). The complexation of the latter with organic cations is well-known and frequently referred to as intercalation.[20] It is found here that the type of the polyanion largely influences film structures and isomerization kinetics of **1** including the rate change at T_c. Effects of the phase transition on fundamental properties such as solute permeability and viscoelasticity of bilayer/PSS[17,18] and bilayer/Mont[21] films have been quite recently studied.

Experimental Section

Materials. 1,3,3-Trimethyl-6′-nitrospiro[indoline-2,2′-2′*H*-benzopyran) (**1**) was purchased from Tokyo Kasei Co. and recrystallized from ethanol. Dioctadecyldimethylammonium bromide ($2C_{18}N^+2C_1$) was obtained from Sogo Pharmaceutical Co. and recrystallized from ethyl acetate. Poly(styrene sulfonate) sodium salt (M_w = 50 000) was obtained from Scientific Polymer Product Co. and used without further purification. Montmorillonite used in this study was the product of Kurimine Ind.

0024-9297/90/2223-0031$02.50/0

Co. (KUNIPIA G-4, cation-exchange capacity (CEC) = 115 mequiv/100 g, and exchangeable cations are Na^+ (87%), Ca^{2+} (10%), and K^+ (3%), according to the manufacturer).

Samples. Polyion complexes were prepared in a method similar to that reported by Kunitake et al.[14] $2C_{18}N^+2C_1$ (0.45 g) was dispersed in 50 mL of distilled water by sonication (Tomy Seiko, Model UR-200P) at 70 °C until a clear suspension was obtained. An amount of polyanion (0.8 molar) dissolved in 30 mL of distilled water was then added dropwise to the above sonicated bilayer solution under vigorous stirring at 70 °C. Montmorillonite was dissolved in water with the aid of sonication for 1 min. On mixing the two solutions, a white precipitate of the polyion complex was immediately formed. The precipitate was filtered off with suction and dried under vacuum. The recovery was ca. 80%. By elemental analyses, the complexed cation/anion ratios were estimated to be 0.97 and 1.09 for the complexes with PSS ($2C_{18}N^+2C_1$-PSS) and montmorillonite ($2C_{18}N^+2C_1$-Mont), respectively.

Transparent cast films of $2C_{18}N^+2C_1$-PSS were obtained by casting the chloroform solutions containing the polyion complex and 1 (0.5–1.0 mol % to the amphiphile) onto a flat quartz or glass plate. The film thickness was approximately 10 μm. The same procedure was applicable also with $2C_{18}N^+2C_1$-Mont,[21] but the resultant cast film was slightly turbid. In most cases the films were then allowed to stand at 60–70 °C (above T_c) at a relative humidity of ca. 100% for 2–3 h. This annealing procedure was essential to give well-structured $2C_{18}N^+2C_1$-PSS film as shown below. Before spectroscopic measurements films were again dried under vacuum.

Measurements. Absorption spectra were measured on Hitachi 808 and Shimadzu 220 spectrophotometers. Cast films were attached to one inner side of a 1-cm quartz cell, and the measurements were achieved at an ambient atmosphere. The quartz cell was electrically thermostated with a Shimadzu temperature controller SPR-5 in the accuracy of ±0.5 °C. Thermal decoloration rates were determined by monitoring the time decay of absorbances at λ_{max}, the visible absorption maximum of PMC. The rate constants were reproducible within the accuracy of 10%.

UV (310 nm < λ < 366 nm) and visible (436 nm < λ) light irradiations were performed using a 500-W super-high-pressure mercury lamp and Corning glass filters.

Phase-transition behaviors of the cast bilayer films were observed by differential scanning calorimetry (DSC) using a DSC-200/SSC-5000 (Seiko Electric Ind. Co.). The heating scan was achieved from −20 to +120 °C at the rate of 2.5 °C/min.

X-ray (Ni-filtered Cu Kα) diffraction patterns of the cast films were measured using a 1.2-kW X-ray camera (Rigaku Denki Co.). Wide-angle X-ray diffraction photographs were taken from piled films with the incident X-ray beam parallel to the film surface. The camera length was determined from the diffraction of Al(111) (diffraction angle $2\theta = 38°27'$).

Results and Discussion

Structures of the Cast Films. The bilayer structures of the $2C_{18}N^+2C_1$-PSS cast films were largely influenced by the annealing procedure described in the Experimental Section. Figure 1 shows the DSC thermograms in the heating process for an as-cast film (curve a) and an annealed one (curve b). Before annealing the endothermic peak was broad and the peak top stayed at a relatively low temperature, 39 °C. In contrast, the annealed film gave a sharpened peak whose top lay at a higher temperature, 49 °C. Furthermore, the transition enthalpy ΔH increased from 2.6 to 10.4 kcal mol^{-1} by annealing. These results show that heating at high humidity brings about better structured bilayer. Heating this film above T_c under a dry atmosphere did not influence the DSC thermograms, indicating that water plays a significant role on the bilayer reorganization. Importance of water for the bilayer formation in the film was also ascertained by dynamic viscoelastic measurements.[22]

For $2C_{18}N^+2C_1$-Mont, the cast film without annealing gave somewhat higher phase-transition temperature,

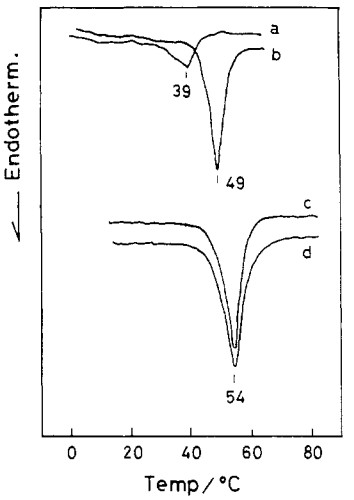

Figure 1. DSC curves for cast bilayer films in the heating process at 2.5 °C/min: (a) as-cast $2C_{18}N^+2C_1$-PSS; (b) annealed $2C_{18}N^+2C_1$-PSS; (c) as-cast $2C_{18}N^+2C_1$-Mont; (d) annealed $2C_{18}N^+2C_1$-Mont.

Table I
DSC and X-ray Data on Bilayer Structures of the Cast Films

film condition	DSC T_c,[a] °C	DSC ΔH, kcal mol^{-1}	X-ray long spacing (d), Å	X-ray tilt angle (θ), deg
		$2C_{18}N^+2C_1$-PSS		
as cast	39.4	2.6	38.4	50[b]
annealed	48.5 (46)[c]	10.4	37.5 (38)[c]	49[b]
		$2C_{18}N^+2C_1$-Mont		
as cast	54.0	9.1	42.4	41[d]
annealed	54.5 (53.9)[e]	10.4	42.4 (48.3)[e]	41[d] (51)[e]

[a] Peak top in the heating scan. [b] Tilt angles were calculated according to the equation $\sin\theta = d/(50\text{ Å})$ (bimolecular length).[23] [c] From ref 17. [d] Interlayer separation = d − 9.5 (thickness of the clay sheet)[20a] Å was used in calculation. [e] From ref 21.

54 °C at the peak top, and a high ΔH (9.1 kcal mol^{-1}). In this case annealing procedure had little effect on the phase-transition properties of the immobilized bilayer (Table I).

Figure 2 presents the X-ray diffraction patterns of the cross section (edge view) of the film sample in which 10–20 pieces of cut cast film (1 × 6 mm) were piled. The arc patterns at small angles show the multilamellar bilayer structure whose membrane plane was preferentially oriented parallel to the film surface. The long spacings (d, Å) corresponding to lamellar thickness and estimated tilt angles (θ) of the amphiphile (angles to the bilayer surface plane) are listed in Table I. The values of the long spacing in our measurements were in good agreement with those reported by others.[15,17] The tilt angles obtained here were in the range of 40–50°, which almost agree with those reported in an X-ray study of the single crystal of dioctadecyldimethylammonium bromide monohydrate (θ = 45°). The degree of order in films of $2C_{18}N^+2C_1$-PSS and $2C_{18}N^+2C_1$-Mont were different as proved by X-ray diffraction patterns shown in Figure 2. With $2C_{18}N^+2C_1$-PSS film, diffractions originating from the lamella were observed only up to second order. On the other hand, diffractions of $2C_{18}N^+2C_1$-Mont film could be detectable more than up to tenth order. Clearly the film prepared with the clay has a more highly ordered lamellar structure than that with the linear polymer. Effect of annealing on the film structures of $2C_{18}N^+2C_1$-PSS could be directly confirmed by X-ray measurements. By anneal-

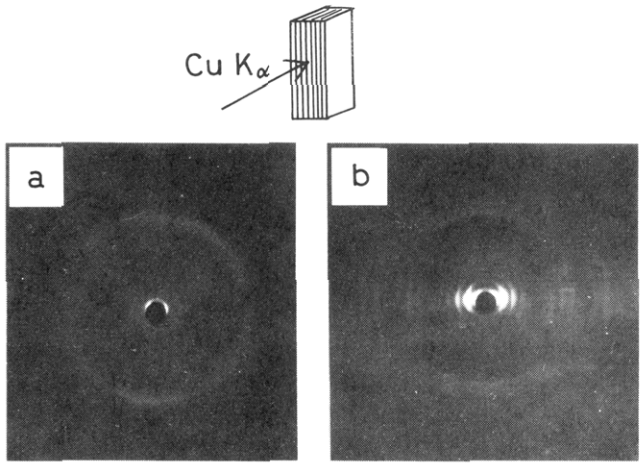

Figure 2. Wide-angle X-ray diffraction patterns of annealed $2C_{18}N^+2C_1$–PSS (a) and $2C_{18}N^+2C_1$–Mont (b) films at 25 °C.

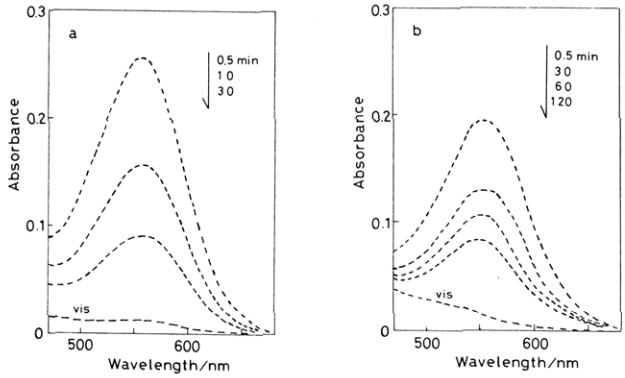

Figure 3. Spectral changes of visible absorption bands of 1 embedded in $2C_{18}N^+2C_1$–PSS (a) and $2C_{18}N^+2C_1$–Mont (b) films in the dark at 35 °C. In each figure times after UV exposure are indicated. vis shows the spectrum after exposure to visible light.

ing clearer diffraction patterns were obtained. With $2C_{18}N^+2C_1$–Mont film, annealing made no significant changes in the X-ray patterns.

Thus, use of the smectitic clay instead of the linear polymer has the advantages that the silicate prevents bilayer structures from disordering in the process of solvent evaporation of casting and that highly ordered lamellar structures are obtainable. Probably stiffness and flatness of the clay sheets assist the growth of ordered lamellar structures.

Photochromic Behaviors of Spiropyrans in Immobilized Bilayers. Spiropyran compound 1 exhibited photochromism in both of the immobilized bilayers complexed with PSS and Mont; i.e., the colorless films turned blue or violet upon UV irradiation and bleached upon visible light irradiation or thermally. Figure 3 shows the changes in visible absorption spectra of 1 in $2C_{18}N^+2C_1$–PSS (a) and $2C_{18}N^+2C_1$–Mont (b) cast films in the dark. λ_{max} of PMC in $2C_{18}N^+2N_1$–Mont film was positioned at 555 nm, which was ca. 10 nm more red-shifted than that observed for $2C_{18}N^+2C_1$–PSS film at 567 nm. Since λ_{max} of PMC is sensitive to medium polarity,[4,7,24] this difference in λ_{max} can be ascribed to the difference in the micropolarity of the matrices surrounding the chromophore. The micropolarities estimated from λ_{max} were approximately equivalent to those in water–1,4-dioxane mixtures of 3/97 and 7/93 for $2C_{18}N^+2C_1$–PSS and $2C_{18}N^+2C_1$–Mont films, respectively.

Thermal Decoloration Kinetics. Kinetic measurements of the thermal isomerization (decoloration) were

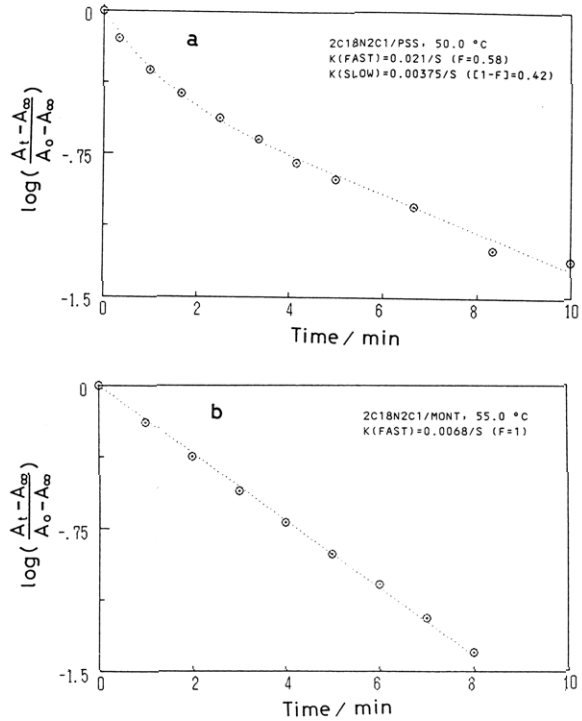

Figure 4. First-order plots for thermal decaying of PMC above T_c in annealed $2C_{18}N^+2C_1$–PSS (a) and $2C_{18}N^+2C_1$–Mont (b) films.

carried out for annealed films. In most cases the thermal decoloration did not obey simple first-order kinetics. In such cases kinetics were analyzed as being the superposition of two, fast and slow, processes. The first-order rate constants were determined by fitting the experimental data to the equation

$$\frac{A_t - A_\infty}{A_0 - A_\infty} = F \exp(-k_{fast}t) + (1 - F) \exp(-k_{slow}t) \quad (1)$$

where A_t, A_0, and A_∞ are the absorbances at λ_{max} at time t, zero, and infinite time, respectively, and F and $1 - F$ are the fractions of PMC's decaying with rate constants k_{fast} and k_{slow}, respectively. Examples of first-order plots are shown in Figure 4. Table II summarizes the rate constants at 30 °C, comparisons of the rates with those in liquid media, magnitude of the rate change at T_c, and activation energies of this reaction in the cast bilayer films.

In $2C_{18}N^+2C_1$–PSS film the first-order plots showed clear deviation from linearity at all temperatures examined (Figure 4a), whereas in $2C_{18}N^+2C_1$–Mont films the kinetics obeyed nearly first order corresponding to slow process at low temperatures below T_c and exactly first order above T_c (Figure 4b) as in solutions. Figure 5 presents the temperature dependence of F, the fraction of the fast process in eq 1. The F value can be a rough indicator of uniformity of the reaction; namely, more homogeneous reaction taking place, F approaches to unity or zero. For the film with the clay, the majority of PMC molecules decayed slowly ($F < 0.2$) at temperatures lower than T_c – 20 °C and decayed fast above T_c ($F = 1$). On the other hand, $2C_{18}N^+2C_1$–PSS film gave $F = 0.4$–0.6, which was hardly influenced by the phase transition.

In Figure 6, temperature dependences of the rate constants of the reaction in annealed $2C_{18}N^+2C_1$–PSS (a) and $2C_{18}N^+2C_1$–Mont (b) films are shown expressed in terms of Arrhenius plots. The rate constants (k, s^{-1}) for both films were increased in a narrow temperature region near T_c. The magnitude of the rate jump at T_c was evaluated by extrapolating the Arrhenius slope from the crys-

Table II
Kinetic Data of Thermal Decoloration of PMC

film	k at 30 °C, s^{-1}		k_{film}/k_{sol}	factor of rate jump at T_c[a]	E_a, kJ mol^{-1}	
	k_{film}	k_{sol}			below T_c	above T_c
$2C_{18}N^+2C_1$-PSS[b]	1.6×10^{-2} (fast)	2.2×10^{-2} [c]	0.72	2.6		
	7.6×10^{-4} (slow)		0.035	4.9	14.2	38.5
$2C_{18}N^+2C_1$-Mont[b]	6.8×10^{-4} (fast)	7.9×10^{-3} [d]	0.086	2.0		
	4.8×10^{-5} (slow)		0.0061	14	53.5	89.9

[a] For the evaluation of the rate jump at T_c, see the text. [b] Annealed films. [c] In water–1,4-dioxane (3/97), λ_{max} = 565 nm. [d] In water–1,4-dioxane (7/93), λ_{max} = 555 nm.

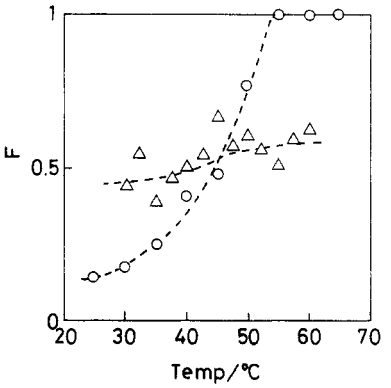

Figure 5. Temperature dependence of F (fraction of fast decaying process in eq 1 in annealed $2C_{18}N^+2C_1$-PSS (△) and $2C_{18}N^+2C_1$-Mont (○) films.

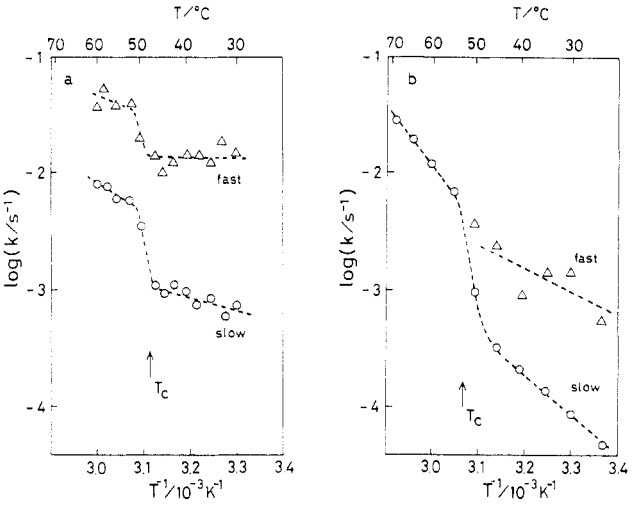

Figure 6. Arrhenius plots for PMC decaying rates of 1 embedded in annealed $2C_{18}N^+2C_1$-PSS (a) and $2C_{18}N^+2C_1$-Mont (b) films. Arrows indicate T_c obtained in DSC measurements.

talline phase to the data at the lowest temperature in the liquid-crystalline phase (Table II).[25] For $2C_{18}N^+2C_1$-PSS film, the reaction rate increased by a factor of approximately 3 (fast process) to 5 (slow process). In the case of $2C_{18}N^+2C_1$-Mont, the reaction was effectively controlled from slow process (below T_c) to fast process (above T_c). With respect to the slow process representing the majority, the rate jump at T_c was approximately 14 times, far exceeding the values in $2C_{18}N^+2C_1$-PSS film.

The ratio of k observed in the films to that in solvents (k_{film}/k_{sol}; Table II) can be assumed to reflect magnitude of restriction of the chromophore mobility imposed by the matrices. Due to the large polarity dependence, k's in the films were compared with those in the solvents of the equivalent polarity as indicated in Table II. In the matrix of $2C_{18}N^+2C_1$-PSS, k_{film}/k_{sol} for the fast component was comparable to unity (0.6–0.7), suggesting that the restriction from the surrounding matrix contributing to this process resembles that from the liquid medium. Rates of slow process were reduced to 0.035, suggesting stronger restriction from the matrix. Reaction rates were even severely suppressed in the matrix of $2C_{18}N^+2C_1$-Mont. k_{film}/k_{sol} was 0.086 for the fast process and 0.0061 for the slow one. As for the slow process this value is 6 times smaller than that in $2C_{18}N^+2C_1$-PSS. The stiff clay sheet seems to suppress the mobility of the amphiphile to further extents than the flexible linear polymer.

The activation energy (E_a) of the reaction was estimated only for the slow process because of less accuracy and scattering of the obtained data for the fast process (Table II). In both film systems, the fluid matrix above T_c gave higher E_a than the rigid state below T_c. This tendency coincides with the observations in amorphous polymer matrices.[1]

The influences of the smectitic clay on the decoloration kinetics of PMC in the bilayer-immobilized films can be summarized as follows: (i) the reaction takes place more homogeneously; (ii) the rate jump near T_c becomes more pronounced; and (iii) the rate is retarded to larger extent. (i) and (ii) may be consistently explained by the degree of order in the film structures; namely, $2C_{18}N^+2C_1$-Mont film has more ordered bilayer lamellar structures. It can be reasonably supposed that highly ordered matrices provide more homogeneous environments for the reaction because contributions of PMC located in disordered or amorphous regions become minor. Concomitantly the observed rate change at T_c becomes larger. Another expected role of the clay is that the location of the chromophore is limited only to the intercalated amphiphile bilayer region as the result of strict exclusion from the silicate layer. This is not the case when a flexible organic polymer is employed: the chromophore can be dispersed not only in the bilayer region but also in the polymer chain part. This localization of sites in the clay film would lead to the same effect on the kinetics.

The origin of the reaction heterogeneity is an important subject to be elucidated. Heterogeneous reactions would be observed if PMC molecules are located at sites of different micropolarity and/or of different matrix structures. The former refers to sites with respect to the bilayer, near the head group or in the hydrophobic long chains, and the latter refers to those in ordered or disordered bilayer structures. If the former factor is predominant, a shift of λ_{max} should be observed in the visible absorption spectra during the decaying process. However, no shifts were in fact observed (Figure 3). Furthermore, as mentioned above on the effect of the clay, the reaction takes place more homogeneously in films having more ordered structures. In consideration of these results, it is plausible that the heterogeneity of the film structure predominates the heterogeneous characters of the reaction. To incorporate photochromic substances into more defined sites of such anisotropic media, designing the chromophore's structure and shape should be important in addition to the matrix structure. Work in this regard is now in progress.

Conclusions

The photochromic reaction of a spiropyran taking place in bilayer-immobilized films consisting of ion complexes between an ammonium amphiphile and polyanions of different types is described. In the casting method adopted in this study, films with more ordered bilayer lamellar structures are obtained by use of the smectitic clay instead of the linear polymer as indicated by X-ray measurements. This difference in the film structure influences the kinetic properties of the thermal decaying of PMC embedded in the films. The film prepared with the clay gives more homogeneous reaction environments for the chromophore than those with the linear polymer. This leads to more drastic changes in this reaction rate at the crystal to liquid-crystal phase transition of the bilayer. To our knowledge, the effect of the phase transition of immobilized bilayers shown in this study is more pronounced than that of the glass transition of amorphous polymer matrices.[1]

Acknowledgment. We are grateful to Prof. Y. Okahata at the Tokyo Institute of Technology for his suggestions in preparation of bilayer-immobilized films and valuable discussions.

Registry No. 1, 1498-88-0; PMC, 16650-15-0; $2C_{18}N^{+}2C_1$, 3700-67-2; montmorillonite, 1318-93-0.

References and Notes

(1) (a) Smets, G. *Adv. Polym. Sci.* **1983**, *50*, 18. (b) Kryszewski, M.; Łapienis, D.; Nadolski, B. *J. Polym. Sci., Polym. Chem. Ed.* **1973**, *11*, 2423. (c) Horie, K.; Tsukamoto, M.; Mita, I. *Eur. Polym. J.* **1985**, *9*, 805, and references therein.
(2) Otruba, J. P.; Weiss, R. G. *Mol. Cryst. Liq. Cryst.* **1982**, *80*, 165.
(3) Ramesh, V.; Labes, M. M. *J. Am. Chem. Soc.* **1987**, *109*, 3228.
(4) (a) Nadolski, B.; Uznański, P.; Kryszewski, M. *Makromol. Chem., Rapid Commun.* **1984**, *5*, 327. (b) Uznański, P.; Kryszewski, M. *Acta Polym.* **1988**, *39*, 613.
(5) Seki, T.; Ichimura, K. *J. Chem. Soc., Chem. Commun.* **1987**, 1187.
(6) Seki, T.; Ichimura, K.; Ando E. *Langmuir* **1988**, *4*, 1068.
(7) Seki, T.; Ichimura, K. *J. Colloid Interface Sci.* **1989**, *129*, 353.
(8) Polymeropoulos, E. E.; Möbius, D. *Ber. Bunsen-Ges. Phys. Chem.* **1979**, *83*, 1215.
(9) Morin, M.; Leblanc, R.; Gruda, I. *Can. J. Chem.* **1980**, *58*, 2038.
(10) McArdle, C. B.; Blair, H. S. *Colloid Polym. Sci.* **1984**, *262*, 481.
(11) Holden, D. A.; Ringsdorf, H.; Deblauwe, V.; Smets, G. *J. Phys. Chem.* **1984**, *88*, 716.
(12) Ando, E.; Hibino, J.; Hashida, T.; Morimoto, K. *Thin Solid Films* **1988**, *160*, 279.
(13) Nakashima, N.; Ando, R.; Kunitake, T. *Chem. Lett.* **1983**, 1577.
(14) Kunitake, T.; Tsuge, A.; Nakashima, N. *Chem. Lett.* **1984**, 1783.
(15) Higashi, N.; Kajiyama, T.; Kunitake, T.; Prass, W.; Ringsdorf, H.; Takahara, A. *Macromolecules* **1987**, *20*, 29.
(16) Kunitake, T.; Shimomura, M.; Kajiyama, T.; Harada, A.; Okuyama, K.; Takayanagi, M. *Thin Solid Films* **1984**, *121*, L89.
(17) Okahata, Y.; Taguchi, K.; Seki, K. *J. Chem. Soc., Chem. Commun.* **1985**, 1122.
(18) Taguchi, K.; Yano, S.; Hiratani, K.; Minoura, N.; Okahata, Y. *Macromolecules* **1988**, *21*, 3388.
(19) Seki, T.; Ichimura, K. *Macromolecules* **1987**, *20*, 2958.
(20) (a) Lagely, Y. *Angew. Chem., Int. Ed. Engl.* **1976**, *15*, 575. (b) Lagely, Y. *Develop in Ionic Polymers*; Wilson, A. D., Prosser, H. J., Ed.; Elsevier Applied Science: London, 1986; Chapter 2. (c) Weiss, A. *Angew. Chem., Int. Ed. Engl.* **1963**, *2*, 134.
(21) Okahata, Y.; Shimizu, A. *Langmuir* **1989**, *5*, 954.
(22) Taguchi, K., personal communication, for the measurement see ref 18.
(23) Okuyama, K.; Soboi, Y.; Iijima, K.; Hirabayashi, K.; Kunitake, T.; Kajiyama, T. *Bull. Chem. Soc. Jpn.* **1988**, *61*, 1485.
(24) Flannery, J. B., Jr. *J. Am. Chem. Soc.* **1968**, *90*, 5660.
(25) In the preliminary report[19] the rate jump at T_c was evaluated as the comparison of experimental data obtained above and below T_c. However, this paper adopts the extrapolation in the Arrhenius plots since normalization to one temperature should provide more meaningful values eliminating the contribution of the temperature coefficient. We thank one of the reviewers for his helpful suggestion on this point.